Improvements to the detection and analysis of external surges in the North Sea

Alexander Müller[1], Birgit Gerkensmeier[1], Benedikt Bratz[2], Clemens Krautwald[2], Olaf Müller[1], Nils Goseberg[2,3], Gabriele Gönnert[1,4]

5 [1]Agency for Roads, Bridges, and Waters Hamburg, Sachsenfeld 3–5, 20097 Hamburg, Germany
[2]Leichtweiß–Institute for Hydraulic Engineering and Water Resources, Technische Universität Braunschweig, Beethovenstraße 51a, 38106 Braunschweig, Germany
[3]Coastal Research Center, Joint Research Facility of Leibniz University Hannover and Technische Universität Braunschweig, Merkurstraße 11, 30419 Hannover, Germany
10 [4]Institute of Geography, Universität Hamburg, Bundesstraße 55, 20146 Hamburg, Germany

Correspondence to: Alexander Müller (alexander.mueller@lsbg.hamburg.de)

Abstract. External surges are a key component of extreme water levels in the North Sea. Caused by low pressure cells over the North Atlantic and amplified at the continental shelf, they can drive water level changes of more than one meter at the British, Dutch and German coast. This work describes an improved and automated method to detect external surges in sea

15 surface time histories. The method is used to analyse tide gauge and meteorological records from 1995 to 2020 and to supplement an existing dataset of external surges, which is used in the determination of design heights of coastal protection facilities. Furthermore, external surges are analysed with regard to their annual and decadal variability, corresponding weather conditions and their interaction with storm surges in the North Sea. 33 % of the 101 external surge occur within close succession of each other, leading to the definition of serial external surges, in which one or more external surges follow less

20 than 72 h after the previous external surge. These serial events tend occur more often during wind–induced storm surges. Moreover, the co–occurrence with a storm surge increases the height of an external surge by 15 % on average, highlighting the importance of the consideration of combined events in coastal protection strategies. The improved dataset and knowledge about serial external surges extend the available basis for coastal protection in the North Sea region.

1 Introduction

25 There is common agreement in scientific debates about the increasing vulnerability of coastal regions due to climate change, which above all leads to increased water levels caused by both long–term effects such as sea level rise and short–term extreme events (Oppenheimer et al., 2019). Institutions and responsible coastal protection authorities constantly have to deal with these changing conditions resulting from long–term sea level rise and short–term extreme water level events. Changes in global (GMSL) and regional mean sea level (MSL) are the most relevant processes causing increased to extreme water levels along

30 the coasts in a long–term perspective. In 2021, the updated IPCC report (Fox–Kemper et al., 2021) reconfirmed that GMSL has risen faster since 1900 than over any preceding century in at least the last 3000 years and will continue to rise over the 21st

century and beyond. Studies on MSL also confirm these trends on a regional scale for the European coastlines, including the North Sea region (Albrecht et al., 2011; Wahl et al., 2013; Steffelbauer et al., 2022), which will be in the focus of this study.

35 In addition to long–term changes, short–term extreme sea levels in particular pose challenges for risk management and coastal protection in low lying coastal regions. For the North Sea coast, extreme water levels are driven by various effects such as wind setup, tides, and intricate local effects. The most common effects related to wind setup are storm surge events, which represent the proportionately largest increases in extreme water levels. The disastrous impacts of storm surges are well known for centuries along the North Sea coast and have been an inherent part of coastal protection strategies. Well–known impacts of climate change are accounted for in recent coastal protection strategies.

40 Besides tides and storm surges, external surges represent an additional phenomenon that generates increased regional extreme water levels in particular along the British, Dutch and German North Sea coast. This phenomenon was first discovered in the 1940s (Corkan, 1948) along the British coastline bordering the North Sea. Increases in water level time histories could not be well explained by local wind setup or tides and were observed to propagate counter–clockwise through the shelf sea similarly to the propagation of tides. Reaching heights of 1.3 m on the British coast and 1.2 m in the German Bight, external surges were

45 also found to occur simultaneously with surge storm events. Combined events like this are already known and confirmed, including the disastrous storm surge event on 16 and 17 February 1962, which caused more than 300 deaths (Koopmann, 1962), or the record storm *Xaver* in 2013 (Fenoglio–Marc et al., 2015).

In practice, those events in which different factors occur at the same time are of particular interest for the design and continuous improvement of coastal protection facilities, because they might produce the most extreme water levels. For this purpose,

50 extensive knowledge about single factors as well as knowledge about effects resulting from superimposing different factors in a combined extreme event, is essential. In contrast to the extensive knowledge available about tides, wind surge and MSL rise, knowledge about the phenomenon of external surges is still relatively rare. To the authors' knowledge, external surges have not been extensively studied with respect to long–term variability and trends, as no dataset of external surges spanning a sufficient period exists. Therefore, this study aims to improve the state of knowledge about external surges by improving the

55 detection of external surges methodologically, building on previous work by Gönnert (2003), and by presenting a novel automated algorithm that is faster and more reliable than previous work. A secondary aim is to apply the novel automated approach to isolate external surges from water level records since 1995 and thus to generate a comprehensive dataset of external surges in the North Sea covering a period from 1971 to 2020.

1.2 External surges: scientific background

60 External surges in the North Sea were first discovered by Corkan (1948) and in the following years also confirmed by other studies in the same area (e.g. Corkan, 1950; Darbyshire and Darbyshire, 1956; Rossiter, 1958) to be progressive anomalies in tide gauge data along the British Coast. Tomczak (1958) investigated a progressive wave at the Dutch and German North Sea coast, which was not recorded at British tide gauges but also coincided with a low pressure cell travelling eastwards over the North Sea. During his analysis of surge residuals, Koopmann (1962) also analysed the propagation of external surges, entering

Natural Hazards
and Earth System
Sciences
Discussions
EGU
Open Access

65   from the northern boundary of the North Sea along the British Isles, the Belgian and Dutch coasts to the German coast and
described a contribution to the high water levels of the devastating flood on 16 and 17 February 1962. This event was also
examined by Bork and Müller–Navarra (2005), who isolated the external surge using a numerical model. The work of Schmitz
et al. (1988), using a numerical model to cover the entire North Sea basin, was able to verify the assumptions about the
generation of external surges in the Northeast Atlantic and their path of propagation into the North Sea. Still, besides the work

70   of Gönnert (2003) who manually investigated external surges in the North Sea over a period of 20 years, no comprehensive
datasets of external surges, identifying their occurrence within observational records are known to the authors.

Similar phenomena to the external surges in the North Sea are known in other shelf seas like the Irish Sea (Brown and Wolf,
2009), the Moreton Bay on the Australian Coast (Treloar et al., 2010) and the Leizhou Bay, which borders the South China
Sea (Liu et al., 2018). As of now, besides the surges in the North Sea, they have only been identified for singular events and

75   have not been statistically assessed over long periods of time. Aside from the lack of analysis stretching longer periods of time,
no comparative study between different sea basins has been conducted so far.

In more recent studies, external surges are often considered in the analysis of storm surge events using numerical models.
While Prandle (1975) used tide gauge measurements of external surges to define boundary conditions for a model of the
Thames estuary, recent models use nested grids to incorporate external surges among other water level oscillations over time

80   and space for varying weather conditions (e.g. Brown and Wolf, 2009; Comer et al., 2017; Ganske et al., 2018). Large–scale
models of the surrounding oceans are used to produce water levels from wind and air pressure data as boundary conditions for
the smaller, more refined models of the actual study area. Ganske et al. (2018) mention external surges as a potential reason
for differences in predicted and modelled storm surge heights at the German Coast. Many of the high storm surge water levels
that occurred during moderate wind speeds coincided with raised water levels at the northern entrance of the North Sea,

85   showing that water level elevations originating from the Northeast Atlantic are an important factor in the prediction of storm
surge heights.

External surges exhibit certain similarities to meteotsunamis, as both are long waves that are generated by air pressure cells
and propagate in shallow water conditions. Both are strongly dependent on Proudman resonance (Proudman, 1929) to amplify
the water level displacement that is expected by estimations like the inverted barometer effect. The generation of

90   meteotsunamis has been studied numerous times in numerical models (Vilibić, 2008; Vennell, 2007, 2010). They are further
amplified by slopes in the ocean bed, especially the continental shelf (Dogan et al., 2021). Meteotsunamis have been identified
around the world, for example in the Adriatic sea (Vilibić, 2008), the Japanese Coast (Kubota et al., 2021), the Yellow Sea
(Kim et al., 2016; Kim et al., 2021) and the Gulf of Mexico (Olabarrieta et al., 2017). They have also occurred in the North
Sea (Jong, 2004; Sibley et al., 2016) but can clearly be differentiated by their characteristics like period, amplitude and their

95   effect on water levels. So far, no comprehensive body of literature on similarities or differences between external surges and
meteotsunamis has been identified.

After careful consideration of existing research on external surges, it can be concluded that external surges can significantly
raise water levels along the North Sea coast. However, available knowledge of external surges is still relatively rare and

translation of knowledge and impacts resulting from external surges into practical approaches, e.g. in terms of concepts for

100   design level for coastal protection facilities, is still very rare. An exception to the missing translation of this knowledge into practice is given by the multi–method approach to calculate design water level of the Free and Hanseatic city of Hamburg that involves detailed analysis of the individual storm surge components tide, external surges, wind surge and their non–linear interactions (Gönnert and Gerkensmeier, 2015; Agency for Roads, Bridges and Waters Hamburg, 2012).

3.1 Objectives

105   In this context, the present work aims to provide a methodology for further external surge research, a comprehensive dataset for the North Sea and to collect existing knowledge about external surges. Not only can the methodology be used to include additional locations in the detection of external surges, but it can also support local authorities in considering external surges for the protection of their communities. The research conducted in this study consists of the specific objectives:

- To improve and automate an existing method of detection of external surges in the North Sea
110   - To extend the knowledge of external surges with respect to their temporal and spatial occurrence and evolution across the basin
- Present a combined dataset of external surges in the North Sea spanning 50 years and highlight the phenomenon of serial external surges
- Discuss implications of enhanced knowledge about external surges in practice, such as coastal protection strategies

115   In the following, this study describes the data used, the method for detection of external surges and the alterations that were made to improve the available dataset on external surges. In Chapter 4, the dataset created by the improved method is analysed concerning the general characteristics of external surges, the accompanying meteorological conditions, and the characteristics of serial external surges. The findings and implications for coastal defence structures are discussed in Chapter 5. In Chapter 6, the conclusions of the proposed methodology and the acquired dataset are drawn and further prospections on the use of this

120   research are given.

3 Materials and methods

3.1 Study area

The study focusses on the North Sea basin, complementing earlier studies about external in this area. The North Sea is a shelf sea connected to the Northeast Atlantic through a 400 km wide opening to the Norwegian Sea and the narrower English

125   Channel, which is 34 km wide at its narrowest point. The depth of the North Sea is on average 95 m but varies between 13 m at the Dogger Bank and 700 m in the Norwegian Trench. Also, the coastal morphology in this focus area is very diverse: fjords at the Scottish and Norwegian coasts, cliffs on the west coasts and marshlands at the southern and south–eastern coasts, which border the Netherlands, Germany, and Denmark. These marsh coasts also include the unique biotope of the Wadden Sea.

In order to capture the dynamics of external surge propagation when entering the North Sea basin, four tide gauges, as shown
in Fig. 1, were selected for the analysis of non–tidal residuals that are distributed over the west coast of Great Britain,
Netherlands, and Germany. The British tide gauges at Aberdeen and Immingham have already been used in several previous
studies (Gönnert, 2003), sometimes alongside additional tide gauges on the British coast (Koopmann, 1962). At Aberdeen tide
gauge, the height of the external surge closely resembles that of the surge action when entering the North Sea, while
Immingham is close to the location where most external surges reach their maximum height. The model of Bork and Müller–
Navarra (2005) determines the maximum height to occur at the estuary *The Wash*, about 55 km south of the Humber estuary,
which coincides with the location of the maximum tidal range on the eastern British coast (ABPmer, 2008). However, the
Immingham tide gauge provides more comprehensive data and shows only small difference to tidal ranges in *The Wash*. Hence,
these first two tide gauges can be assumed to be representative of important characteristics of external surges. The tide gauge
in Cuxhaven has been regularly used as reference tide gauge in German coastal protection considerations as it provides a
continuous data series (continuous record is available since 1918, earlier data available for specific events), which is nearly
undisturbed (e.g. by man–made impacts), and is influenced neither by barriers like the East Frisian Islands nor by the Elbe
estuary fluxes. These three tide gauges have also been used in the study by Gönnert (2003), which serves as a benchmark for
the present study. Additionally, the present study uses the tide gauge at Texel because it is located in almost even distance to
Immingham and Cuxhaven and can thus supplement information about the propagation of external surges after they reached
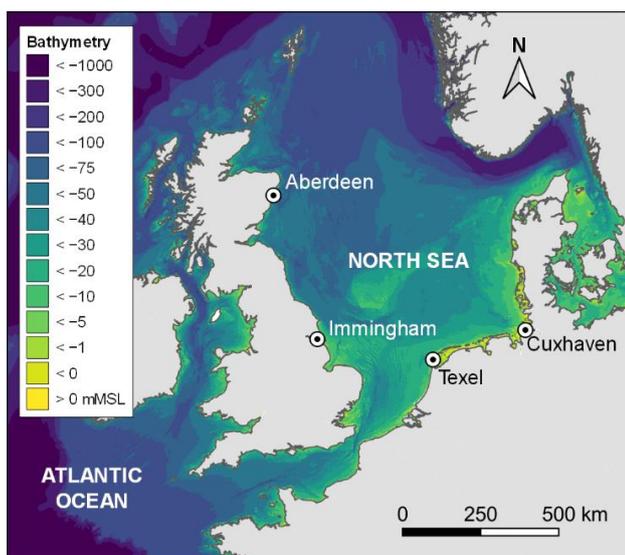their maximum height near Immingham.

Figure 1: Study area and locations of the tide gauges. Bathymetry was provided by EMODnet Bathymetry Consortium (2020).

5

Table 1: Location, offset to NAP, data sources and percentage of flagged data (flags from the data providers, missing and unreasonable values) for each measurement station.

Tide gauge	Lat.	Lon.	Offset tide gauge zero (TGZ) to NAP [m]	Tide gauge data source	Tide gauge data time steps	Weather data source	Weather stations	Weather data time steps	Flagged data points [%]	Additional information
Aberdeen	57° 08' 38.6" N	02° 04' 48.5" W	−2.45	NOC British Oceanographic Data Center (2021)	15 min quality checked	-	-	-	2.0	
Immingham	53° 37' 51.7" N	00° 11' 9.7" W	−4.10			-	-	-	2.2	
Texel	53° 07' 14.2" N	4° 43' 59.4" E	0.00	Rijkwaterstaat (2021)	10 min quality checked	Koninklijk Nederlands Meteorologisch Instituut (2021)	De Kooy	1 h	4.4	Two larger gaps from 11 January to 22 November 2002 and 16 June to 2 July 2020
Cuxhaven	53° 52' 03.7" N	8° 43' 02.7" E	−5.03	1995–1997: Wasserstraßen– und Schifffahrtsverwaltung des Bundes (2021a); 1998–2020: Wasserstraßen– und Schifffahrtsverwaltung des Bundes (2021b); Astronomical tides: Federal Maritime and Hydrographic Agency (2021)	1995–1997: 1 h; 1998–2020: 1 min; Astronomical tide: 10 min quality checked	DWD Climate Data Center (2021)	Wind: UFS Deutsche Bucht, UFS TW Ems, Helgoland; Air pressure: Cuxhaven	1 h quality checked	2.4	

3.2 Data acquisition and processing

All data used in this study were provided by local authorities, mostly through open access data portals. To receive uniform input data, all data were filtered to contain only hourly measurements, and tide gauge data as well as astronomical tides were transformed to be in reference to the Amsterdam Ordnance Datum (NAP). Missing or highly unlikely data like wind speed above 35 m s^{-1} and air pressure above 1050 hPa or below 950 hPa were flagged and combined with the flags from the quality checks of the data providers. Flagged values are still used in the calculation of residuals, as the flags can also indicate successfully verified data. Overall, of the 227928 data points per location, the fractions flagged as missing or unreasonable are given in Table 1.

The weather data used to hindcast wind setup at the tide gauges at Texel and Cuxhaven consists of:

- Mean wind direction (averaged over the last 10 min before the timestamp)
- Mean wind speed (averaged accordingly)
- Air pressure reduced to sea level.

3.3 Methodological approach to identify external surges

To isolate external surges from hydrographic records, all other major components have to be eliminated. The methodology was developed by Gönnert (2003), but was adapted for this study to make the time steps independent from tidal cycles and therefore enable a more refined analysis.
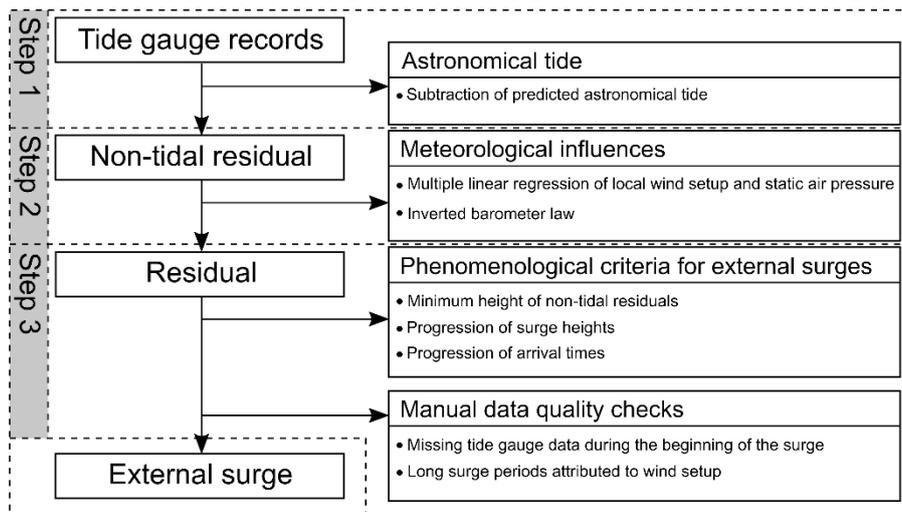

Figure 2: Schematic representation of the process to identify external surges.

Figure 2 gives an overview over the general steps in this process. While Gönnert used the average residual between high and low water, resulting in time steps of 6.25 h, here the time steps are shortened to 1 h, allowing more precise assertions of the duration, height, and timing of the events. The process consists of three basic steps: each eliminating one contributor to water

levels: first the astronomical tide, second the meteorological influences. The methodology of this step varies between the tide gauges due to different local and regional bathymetry and time lag between wind and water level maxima (Proudman and Doodson, 1926; Dibbern and Müller–Navarra, 2009). Third, other phenomena that cause residuals are eliminated and the detected events are reviewed for flawed data.

175   First, the non–tidal residual is determined in Eq. (1) by the astronomical tide (h_{astro}) and the observed water level (h_{obs}):

$$\Delta h_i = h_{i,obs} - h_{i,astro} \tag{1}$$

In step 2, the influence of meteorological factors on the non–tidal residual during external surges has to be discussed to derive the wind setup and the residual individually. For the British tide gauges, Rossiter (1959) developed empirical forecast formulae based on air pressure gradients from five sample point over the North Sea and Northeast Atlantic, which can be attributed to wind directions and speeds. For the Aberdeen tide gauge, he concluded that residuals mainly depend on:

180
- Local air pressure deviations, using the base value of 1012 hPa
- North–eastern winds over the North Sea, with a time lag of 3 h
- Return surges that occur approximately 15 h after southern winds over the northern North Sea
- Western winds over the North Atlantic, with a time lag of 9 h, causing or driving external surges

Due to the different main wind direction, it is highly unlikely, that more than one of the latter three factors influence water
185   levels in Aberdeen simultaneously in a significant amount.

For the Immingham tide gauge, Rossiter (1959) concluded that the following parameters influence the residuals the most:

- The residual at Aberdeen with a time lag of 5 h
- North–eastern winds over the North Sea with a time lag of 6 h

The first accounts for local air pressure as well as external surges propagating southwards along the British coast. As the
190   entrance of external surges is hindered by eastern winds, these two main factors do not coincide very often. For these two British tide gauges it can therefore be concluded that wind setup does not need to be accounted for during the detection of external surges. The influence of other factors like water and air temperature or wind setup should be taken into consideration during the interpretation of surge heights, nonetheless.

For the tide gauge at Cuxhaven, Müller–Navarra and Giese (1999) developed an empirical forecast model using various
195   meteorological input factors like x and y components of the quadratic and cubic wind speed, air and water temperature gradients, static air pressure and short term air pressure changes as well as increases in water levels spanning multiple tide phases or stemming from the Atlantic. Wind setup tables, using wind speeds and directions as input, were provided by the Federal Maritime and Hydrographic Agency (BSH) and used to hindcast the expected wind setup. These table group the measurements by two criteria, to account for non–linear interactions between tide and wind setup:

200
- Tidal phase: Based on the height of the hindcast astronomical tide, the data points are split into high (HW, $a_{astro} > 0\ cm$ above NAP) and low water phases (LW).

- General wind direction (onshore or offshore): wind directions are split orthogonally to the main wind direction. The main wind direction, which produces the highest wind setup was determined to be around 295° at Cuxhaven (Annutsch, 1977; Gönnert, 2003). Winds between 20° and 200° are offshore wind, resulting in negative wind setup in the German Bight.

The time lag between wind measurements and water level deviation is given by Müller–Navarra and Giese (1999) at 3 h. For the influence of static air pressure, the *inverted barometer law* (IBL) is used. It states that a decrease in air pressure by 1 hPa correlates linear to an increase in water level by 1 cm (Koopmann, 1962). Even though this correlation is simplified and can vary depending on local factors (Ponte and Gaspar, 1999; Müller–Navarra and Giese, 1999; Olbert and Hartnett, 2010), it is found to be in good agreement with the conditions at Cuxhaven. A simplified analysis of wind setup at Cuxhaven, using only wind and air pressure measurements, determined linear factors between 0.9 and 1.25 cm hPa^{-1}, depending on tidal phase and main wind direction. The other predictors of the forecast model are omitted due to lack of data (air and water temperatures) or because they anticipate the effect of external surges, as they can last several tidal phases and enter the North Sea from the Atlantic.

Table 2: Functions to produce MLR input

j	Function g_j	Unit of regression factor a_j	Description
0	1	cm	Constant factor
1	$f^2 \sin \beta$	cm (m s^{-1})$^{-2}$	Quadratic wind velocity
2	$f^2 \cos \beta$		
3	$f^3 \sin \beta$	cm (m s^{-1})$^{-3}$	Cubic wind velocity
4	$f^3 \cos \beta$		
5	$p - 1015 \, hPa$	cm hPa^{-1}	Static air pressure

At the Texel tide gauge, a simplified method of this forecast model, which was introduced by Dibbern and Müller–Navarra (2009), is used to calculate wind setup tables and the air pressure coefficient. The method defines the water level as the weighted sum of multiple terms depending on meteorological measurements. The functions and units of the six terms are given in Table 2. Function 1 is a constant term for the difference between the neutral sea state and MSL. Functions 1 and 2 two are the orthogonal components of the quadratic wind stress, function 3 and 4 add the cubic wind stress. Function 5 accounts for static air pressure and uses the same assumption as the IBL. The weighted sum of these terms gives a prediction of the measured non–tidal residual. In Eq. (2), deviations from the measured height are incorporated by an error term:

$$\Delta h_i = \sum_{j=0}^{J} a_j g_j(\boldsymbol{x}_i) + e_i \tag{2}$$

A multiple linear Regression (MLR) optimizes the regression factors for the least square error. The total of the squared errors is defined in Eq. (3) which is taken from the detailed description of the procedure in Müller–Navarra and Giese (1999).

$$\chi^2(\boldsymbol{a}) = \sum_{i=1}^{I} e_i^2 = \sum_{i=1}^{I} \left(\Delta h_i - \sum_{j=0}^{J} (a_j g_j(\boldsymbol{x}_i))^2 \right) = min \qquad (3)$$

Table 3: Overview of the remaining data points available for MLR and validation for Texel and Cuxhaven subdivided into tide phase groups.

Tide gauge	Tide phase	Data points used for MLR	Data points used for validation
Texel	HW offshore	19841	70071
	HW onshore	25947	
	LW offshore	17378	61358
	LW onshore	22866	
Cuxhaven	HW	-	65181
	LW	-	55471

Data is again grouped into four groups by tidal phase and wind direction. The MLR is conducted for each group individually.
230 Data from 1995 to 2004 is used to determine the regression factors so that independent validation of the regression results can
be conducted using the 2005 to 2020 data. The 2005 to 2020 data is also used for the Cuxhaven tide gauge to verify the wind
setup tables of the BSH. Table 3 gives the number of data points used in each regression and validation. Flagged data points
are not included in the regression data, as the flags do not accurately distinguish between verified or corrected and flawed data.
Data points with wind speeds above 20 m s^{-1} are not included as well, because these rather rare events show great variability
235 and have strong influence on the regression factors, causing an overall worse hindcast if included.
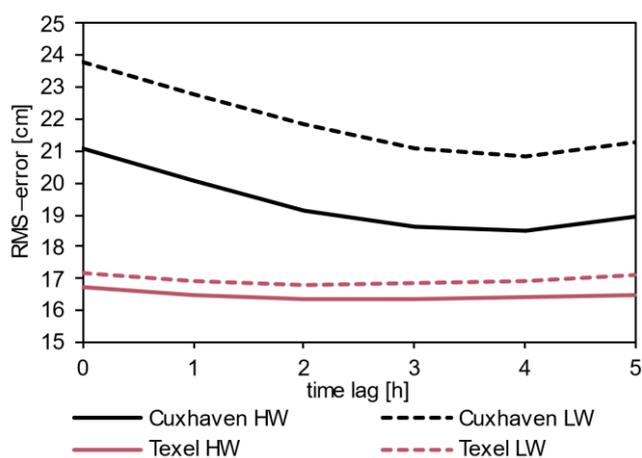

Figure 3: RMS–error depending on the time lag between measured winds and wind setups at the tide gauges in Cuxhaven and Texel.

For the Texel tide gauge, the unknown factors of main wind direction and time lag between wind and water level have to be
determined as well. This is achieved by multiple runs of the MLR using different main wind directions and time lags and the

240   calculation for the root mean square error (RMSE). The limit between on– and offshore wind is found to be around 20° and 200° degree as well, which is close to the general orientation of the coast of the island Texel. The optimization of the time lag is shown in Fig. 3, which determines a time lag of two hours. It also shows that the time lag for Cuxhaven of three hours is accurate for high water phases, but for low water phases a slightly better hindcast is achieved with a time lag of four hours.

Table 4: Regression factors a_i for the tide gauge at Texel and statistical significance of each component.

Component i	HW				LW			
	Onshore	Sig.	Offshore	Sig.	Onshore	Sig.	Offshore	Sig.
0	−2.086	< 0.001	−0.619	< 0.001	−2.994	< 0.001	−1.576	< 0.001
1	−0.574	< 0.001	−0.462	0.000	−0.622	< 0.001	−0.456	< 0.001
2	0.329	< 0.001	0.295	< 0.001	0.307	< 0.001	0.298	< 0.001
3	0.011	< 0.001	0.013	< 0.001	0.017	< 0.001	0.009	< 0.001
4	−0.011	< 0.001	−0.007	< 0.001	−0.013	< 0.001	−0.008	< 0.001
5	0.862	0.000	0.805	0.000	0.909	0.000	0.915	0.000

245

Table 4 lists the regression factors for the optimal main wind direction and time lag for the tide gauge at Texel and their statistical significance for the four groups of data points. The air pressure coefficient for example varies between 0.8 and 0.92, meaning that the dependence on static air pressure is more uniform than in Cuxhaven but slightly smaller than predicted by the IBL.

250   In Eq. (4), the regression factors of the components 0 to 4 are used to compile wind setup tables similar to those of the BSH:

$$\Delta h_{W,i} = a_{0,i} + \left(a_{1,i} \sin \beta_i + a_{2,i} \cos \beta_i\right) f_i^2 + \left(a_{3,i} \sin \beta_i + a_{4,i} \cos \beta_i\right) f_i^3 \tag{4}$$

Additionally, the water level deviation due to air pressure is calculated in Eq. (5):

$$\Delta h_{AP} = a_{5,i}(p - 1015\ hPa) \tag{5}$$

For Cuxhaven, where the IBL is used, a_5 equals 1 cm hPa^{-1}. These two meteorological effects are used in Eq. (6) to calculate the residual in Cuxhaven und Texel:

$$\Delta h_R = \Delta h - \Delta h_W - \Delta h_{AP} \tag{6}$$

255   To assess the quality of the hindcast, the calculated wind setup including the effect of static air pressure is plotted against the measured wind setup for both tide gauges and grouped by tidal phases in Fig 4, using the verification time period. Hindcast and measurement are in overall good agreement, but show the tendency of hindcasts underestimating wind setup, which is more pronounced at Texel tide gauge. This is probably due to the reduced set of predictors of wind setup. The method was tested for the British tide gauges as well but did not produce sufficient results, probably due to the wrong set of key predictors.

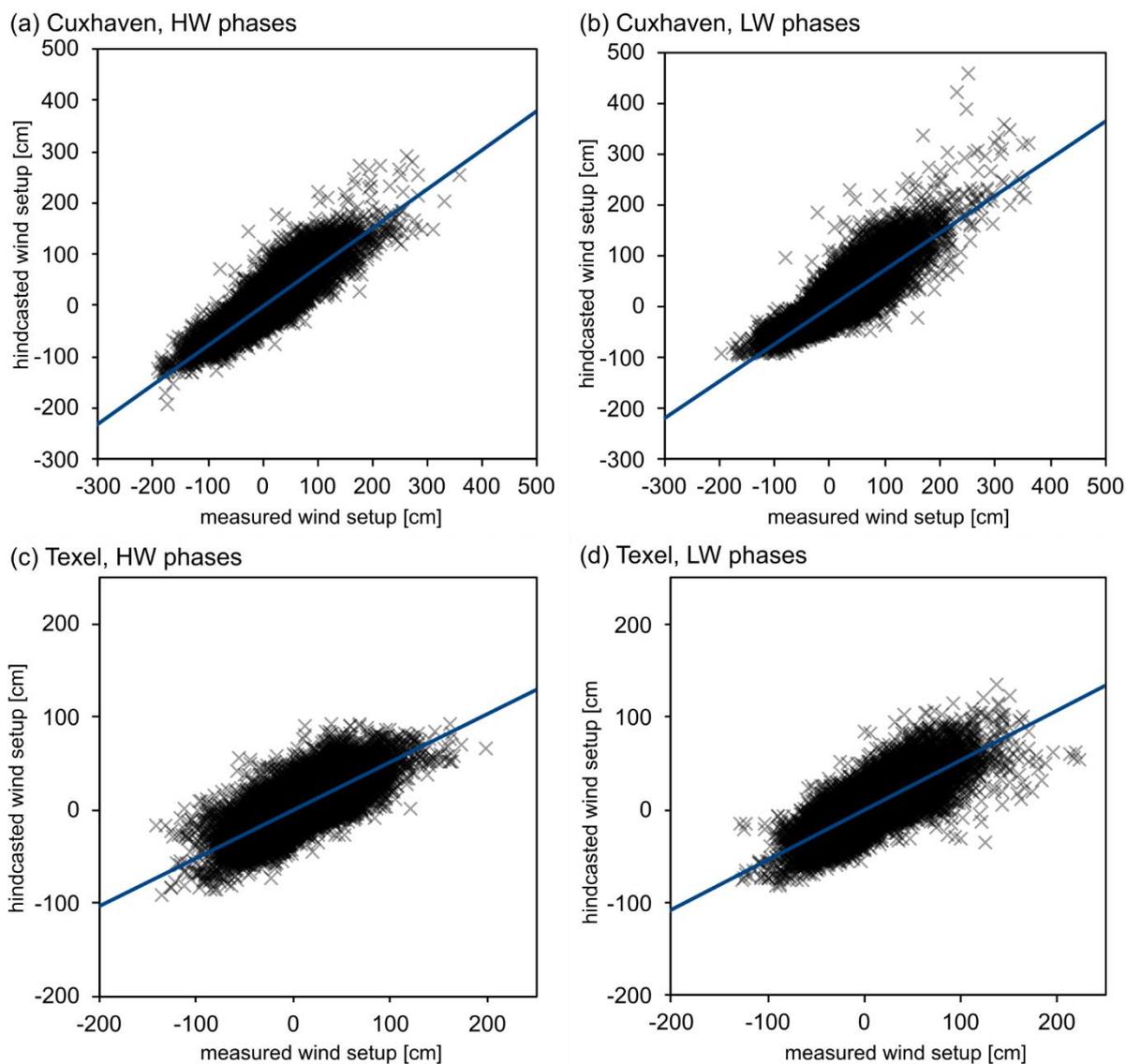260   Approaches to improve the wind setup for all locations are discussed in Sect. 5.

Figure 4: Comparison of hindcasts and measurements of wind setups at Cuxhaven (a & b) and Texel (c & d).

To mitigate the effects of spikes or troughs and to further account for the delayed reaction of wind setup, the wind setups are
265 averaged over three hours from two hours before the timestamp to one hour after the timestamp. For Cuxhaven, the wind setup
is calculated from the winds from 5 h to 2 h before the water level measurement. In step 3, the residuals are filtered for external
surges based on the following conditions proposed by Gönnert (2003):

- The non–tidal residual in Aberdeen is greater than 40 cm.
- Surge heights generally increase from Aberdeen to Immingham, caused by local winds, with a maximum decrease of
270 10 cm.

- The arrival at Immingham is at least 2 h later than at Aberdeen, but no more than 5 h later. The time of arrival is defined as the time when the non–tidal residual is over 10 cm in height.

Afterwards, a manual quality check of the filtered surges is conducted. A total of four surges were eliminated due to one of two reasons:

275
- Missing tide gauge data during the beginning of the surge in Aberdeen or Immingham. The height or the offset of the surge may be influenced by these missing values.
- Long surge periods that can be attributed to wind setup in Aberdeen and Immingham

3.4 Sensitivity analysis

Criteria for external surges are assessed by varying the minimum height at Aberdeen and the maximum offset between
280 Aberdeen an Immingham. The minimum height in Aberdeen is found to be suitable for the uncertainties of the hindcast of tides and wind setup. If the minimum height is reduced by 10 cm, more than 50 % of the additionally detected surges cannot clearly be differentiated from fluctuations in residuals due to wind setup and other factors. For an increase of the temporal offset from 5 h to 7 h, the error rate is only 24 %, meaning that 76 % of the additionally detected surges match external surges in their general behaviour like heights at the four tide gauges and periods. However, to maintain comparability between this
285 study and the study conducted by Gönnert (2003), these surges are not included in the dataset. Moreover, external surges have to be studied further to discern, whether an offset of 7 h between Aberdeen and Immingham is physically possible.

4 Results

4.1 The phenomenon of serial external surges

Overall, 65 external surge events were identified between 1995 and 2020 (labelled DataSet2); the statistical base parameters
290 of this new dataset are listed in Table 5. Several of those events consist of more than a single external surge and are identified as a sequence or series of external waves in the residual water level oscillations. Figure 5 gives examples of both, a single external surge (a) and an event consisting of three external surges (b), arriving with gaps of 22 h between the first and second surge and 43 h between the second and third surge. For those events, it is possible that they depend on the same meteorological origin, caused by storm systems in the Northeast Atlantic. Moreover, they can interact with each other in the North Sea, as
295 they can remain there for more than 48 h depending on their celerity and wavelength. This can also be seen in Fig. 5b): during the arrival of the second external surge at Aberdeen, the residual at the Cuxhaven tide gauge is still at around 30 cm caused by the first external surge. It also shows possible effects of the interaction of the first two surges: while the two external surges are mostly uniform and of similar height at Aberdeen and Immingham (the peak height varies by around 15 cm), the second external surge is 30 cm higher at Texel and 50 cm at Cuxhaven. To verify whether this behaviour is caused by interactions of
300 the two external surges or other influences, more detailed studies should be conducted using numerical models or residuals at

other tide gauges. In this study, the term "serial external surges" is used for series of identified external surges in close succession. In total, 101 external surges were found in 65 external surge events. Some of those external surges were also detected by the automated detection but grouped with other external surges, others do not match the required height or offset between Aberdeen and Immingham. Since they occurred shortly before or after a detected external surge, they are also included

305 in the dataset.

Table 5: Total number of external surge events and external surges in the datasets.

	DataSet2	DataSet1	Combined datasets
Begin	1995	1971	1971
End	2020	1995	2020
No. of years	26	21 [a]	46 [a]
External surge events	65	63	126 [b]
per year	2.50	3.00	2.74
Containing 1 surge	42	54	96
% of all events	66.7	85.7	76.1
Containing 2 surges	11	8	19
% of all events	17.4	12.7	15.1
Containing $\geq$ 3 surges	10	1	11
% of all events	15.9	1.6	8.7
External surges	101	73	172 [b]
per year	3.88	3.48	3.74

[a] deducting four years with missing data (1974–1977)

[b] deducting two events that are part of both datasets (18 January & 1 February 1995)
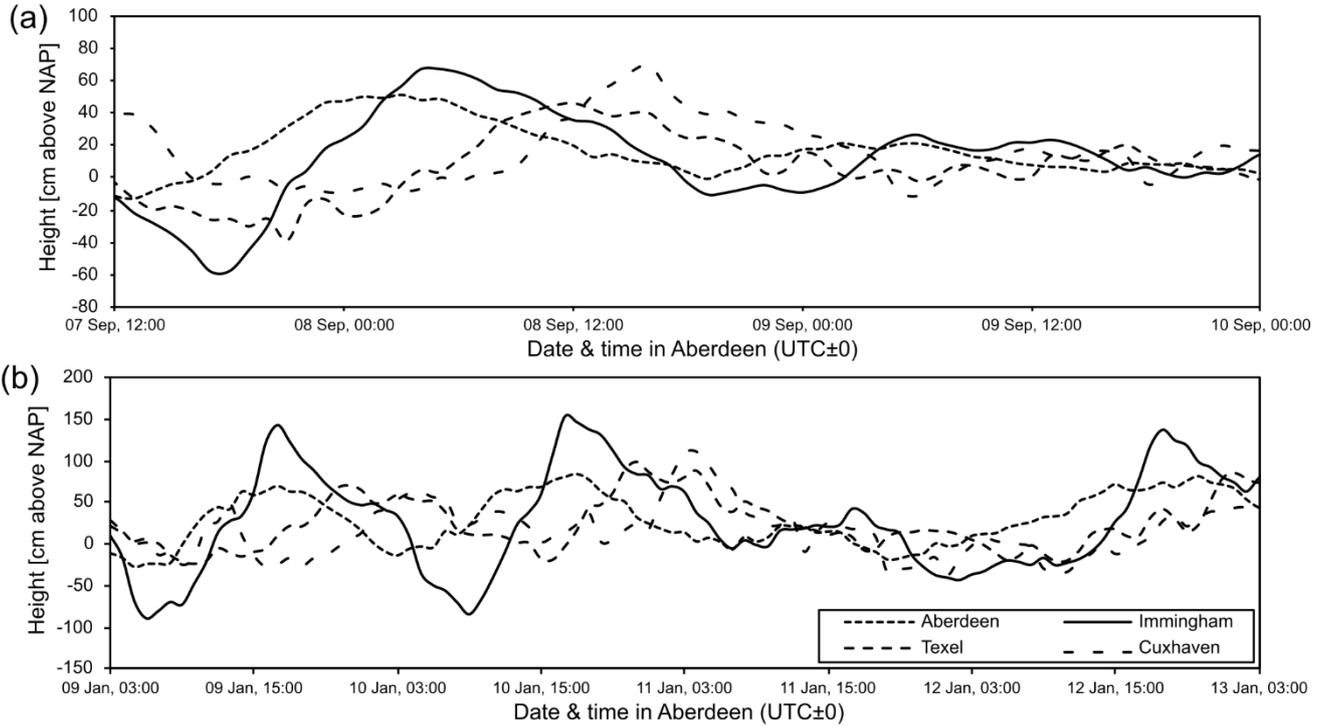
310

Figure 5: Height of the non–tidal residual (at the gauges in Aberdeen & Immingham) and the residual (at Texel & Cuxhaven) for examples of an external surge on 7 and 8 September 2000 (a) and a serial external surge on 9–13 January 2015 (b).
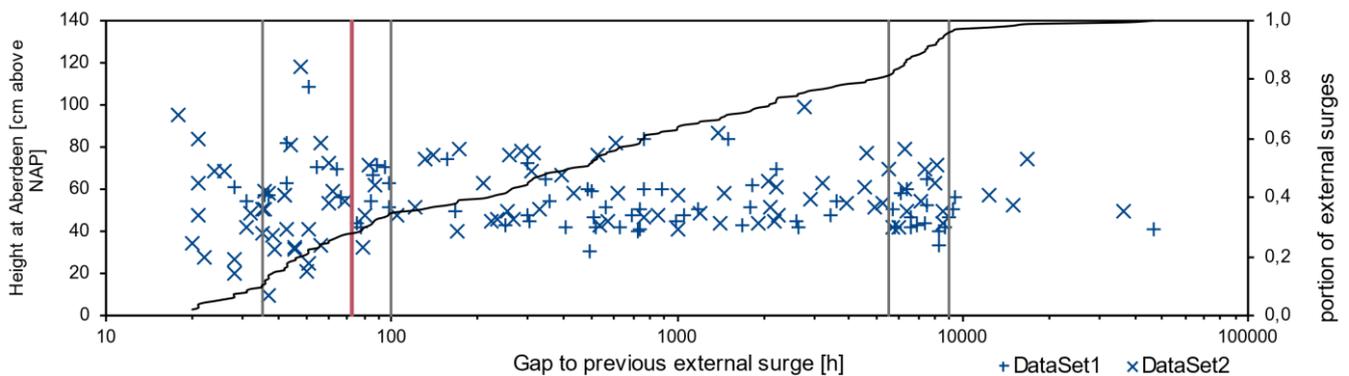

315 **Figure 6: Height of the external surges (combined datasets) over the time gap to the previous surge and the sum line of external surges depending on the gap to the previous surge. Two areas of stronger increases can be seen (highlighted by the grey lines): between 35 and 100 h and between 5500 and 9000 h. The first shows the occurrence of serial external surges, the second is due to the lack of external surges in spring and summer, resulting in similar gaps between the last surge in winter and the first surge in autumn. The red line shows the threshold of 72 h for serial external surges.**

320 Figure 6 shows the heights of each external surge and the gap to the previous external surge (please note the logarithmic scale).

Additionally, the sum line of events depending on their gap to the previous surge. A closer inspection of the sum line reveals

15

two frequency peaks: one peak exists for external surges occurring less than 100 h after the last surge and the second peak is for a timespan between 230 and 375 days (5500 and 9000 h). The second peak originates from the very rare occurrence of external surges during spring and summer months, resulting in similar timespans between the last surge in winter and the first

325   surge in the following autumn. The first peak however indicates that the frequency of serial external surges is way higher than would be expected by the random close occurrence of two independent external surges. A threshold duration of 72 h is chosen, as the definition of serial external surges should not only include their increased occurrence, but also their origin (the same or closely succeeding low pressure cells) and their possible impact (interaction with each other and modulation of storm surges). The occurrence of serial external surges has not been addressed in the recent literature so far.

330   In the context of coastal protection, serial external surges should also be analysed as interdependent waves, since they can influence peak water level in a couple of different ways depending on the timing between high waters, maximum wind setup and external surge peaks. A single storm surge spanning over multiple tide cycles might well be influenced by two or more external surges in close succession, e.g., resulting in higher peak flood elevations as compared to cases where external surge events are absent. The assumption of interactions between these external surges cannot be verified in this study as it requires

335   more detailed analysis with higher spatial and temporal resolutions, possibly including numerical simulations.
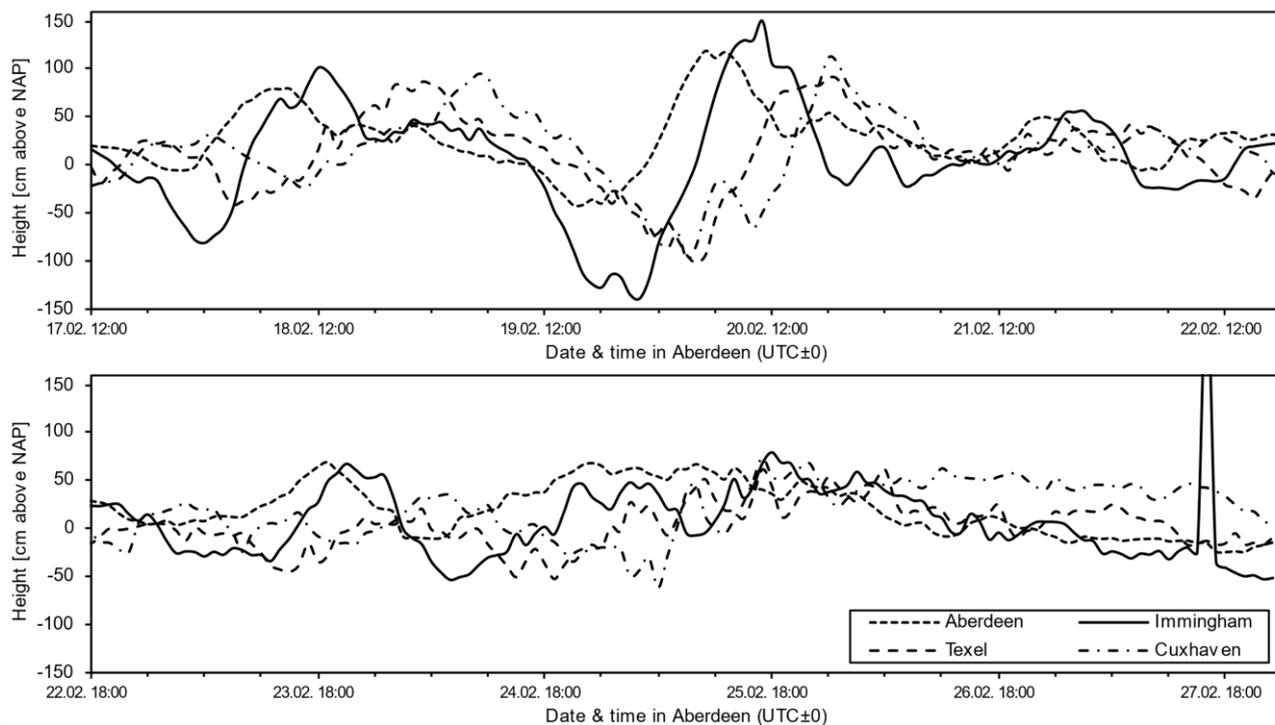

Figure 7: Height of the non–tidal residual (at the gauges in Aberdeen & Immingham) and the residual (at Texel & Cuxhaven) for during the serial external surges from 17 to 27 February 1997. The fourth surge, starting on 22 February at 06:00 in Aberdeen does not reach the required height limit. However, if the preceding troughs are considered, this surge reaches 39 cm in Aberdeen and
340   **48 cm in Immingham and can therefore be considered as an external surge. The spike in Immingham around 27 February 15:00 is due to uncorrected flawed data.**

16

In DataSet2, a third of the external surge events consisted of more than one surge. Of those, 11 events contain two surges, the other ten contain three or more surges. One special event can be found in February 1997: from 18 February onwards, six consecutive external surges were detected, all within 72 h of each other. The calculated residuals for this event are plotted in

345   Fig. 7. This series of surges lasted until 27 February. From 28 February to 3 March two additional surges can be seen in the residuals that loosely resemble external surges but do not match the criteria defined previously. The weather conditions in Northwest Europe were consistent during the period with westerly wind and low–pressure cells over the Atlantic, which match the conditions that Gönnert (2003) found to be the most prominent during the detection of external surges.

The dataset from Gönnert (2003) (labelled DataSet1) was not previously analysed with regards to serial external surges. This

350   study hence uses that dataset with a focus to detect additional serial surge events, appending them to these found in the 1995 to 2020 dataset. 73 external surges can be grouped into 63 events. In eight cases or 12.7% of the external surge events two external surges were detected less than three days apart, which is slightly less than in DataSet2. By contrast, only one event containing three surges is found, so that the overall percentage of serial external surges is lower in this dataset. This aberration might be due to the different time steps of the analysis and cannot be interpreted as a significant trend. All in all, 30 serial

355   surge events are identified, of those 19 consist of two surges and three of four or more (cf. Table 5).

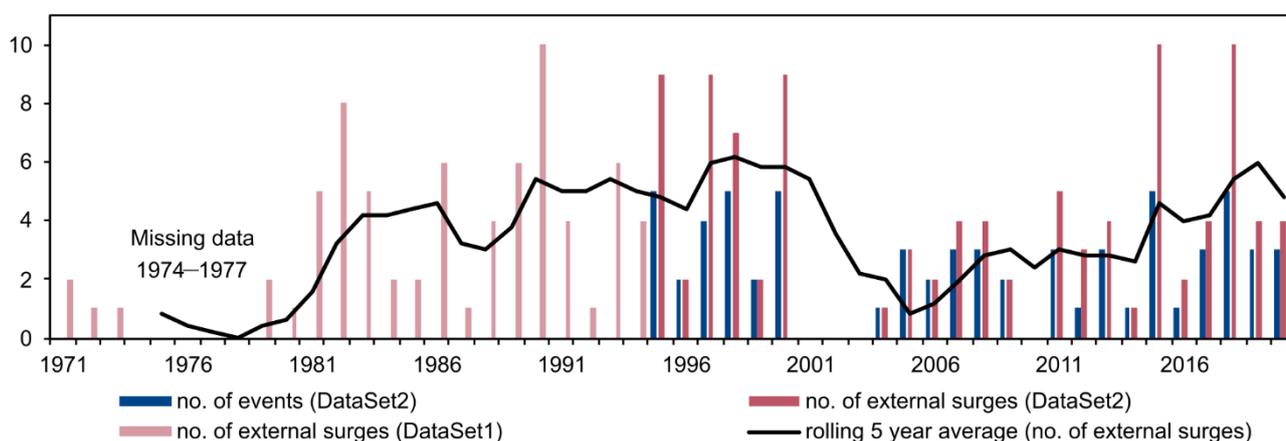### 4.1 Frequency and height of external surges in the North Sea

Figure 8: Number of external surges per year and rolling 5 year average, combination of this study and data from Gönnert (2003). The 5 year average is accurate from 1983 onwards, as previous values include years with missing data. From 1995 onwards, the

360   **number of events is also shown, which counts serial external surges as a single event.**

Figure 8 shows the number of external surges per year for both datasets and their rolling 5 year average. In comparison to the external surges found by Gönnert (2003), the total number of external surges increases while the number of external surge events decreases slightly. The increased number of external surges can mainly be explained by the higher temporal resolution that enables a clearer distinction between single external surges, and the focus on serial external surges. On the other hand, the

365   decrease in the number of external surge events is rather small and can mainly be attributed to the period from 2001 to 2006,

when only six events were detected. Due to this variability in their occurrence no significant trend can be determined, as linear, polynomial, or logarithmic trend lines predict an increasing, constant, or falling number of external surges respectively.
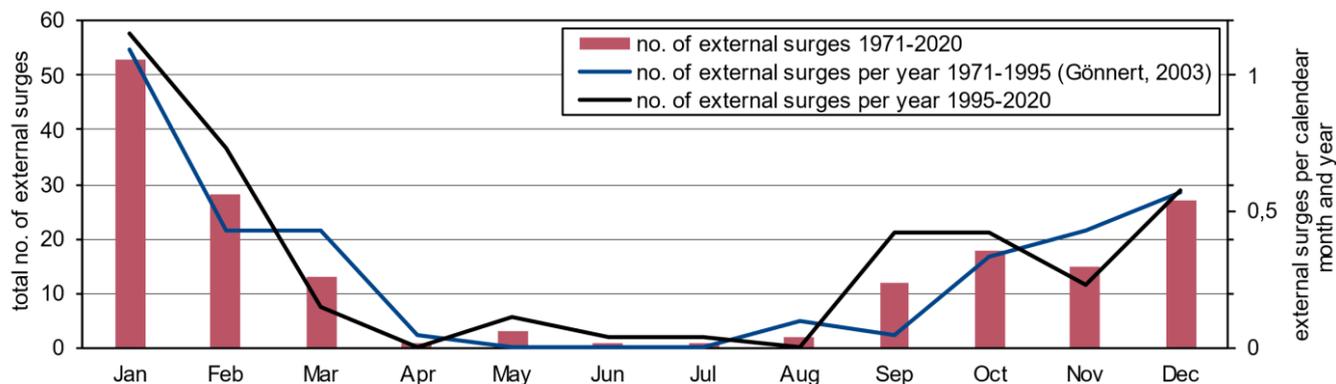
Figure 9: number of external surges per calendar month, the data from Gönnert (2003) contains a data gap from 1974 to 1977, which does not influence the monthly distribution, as whole years are missing.

The distribution of external surges over the year (cf. Fig. 9) – an important distribution with respect to its co–influence with wind surge effects in coastal waters – is not equal but shows a strongly increased occurrence during autumn and winter months with January having the highest number of external surges. Only eight of the 172 external surges from DataSet1+DataSet2 occurred during the spring and summer months from April to August. The comparison of distributions between the two datasets shows a tenfold increase of external surges in September and a decrease of 65 % in March. This may hint towards a shift of the main external surge season to start earlier in the year but also end earlier. As of now, the datasets do not span a sufficient timeframe to verify this assumption. A one–tailed t–test (using the day of arrival after 1 July) found earlier arrival by six days between DataSet1 (M= 183.0, SD= 50.5) and DataSet2 (M=177.1, SD= 63.3). However this difference was not found to be significant, t(170)= 0.681, p=.248 > 0.05.
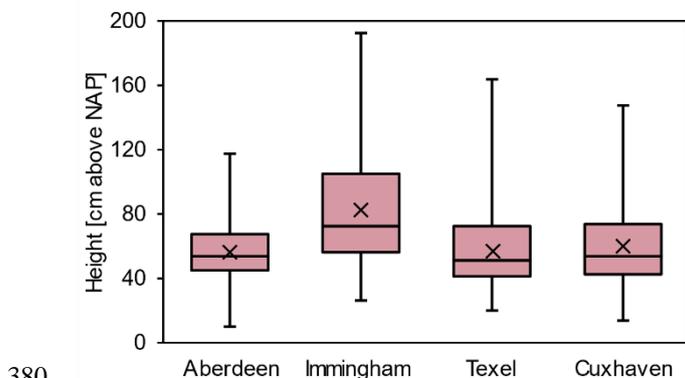

Figure 10: Boxplot of the heights of external surges in Aberdeen, Immingham, Texel, and Cuxhaven from 1995 to 2020.

The height of the external surges matches previous studies and simulations (Schmitz et al., 1988; Gönnert, 2003; Bork and Müller–Navarra, 2005). Figure 10 shows boxplots of the heights of the recorded external surges. Beginning with an average

18

height of 56 cm in Aberdeen, the external surge height increases along the British coast and reaches 83 cm in Immingham.

385   During their propagation along the southern and south–eastern coast of the North Sea, their averaged height decreases to 57 cm and 60 cm at Texel and Cuxhaven gauges, respectively. Nonetheless, the maximum height of the surges can reach 100 cm in Aberdeen with a single even higher event with 118 cm. The highest overall surge height was recorded in Immingham with 192 cm. At Texel and Cuxhaven, the highest events also more than double the average height with 164 cm and 148 cm respectively. The most extreme event in Texel should be further assessed as it is almost 60 cm higher than the second highest.

390   This exceptionally high external surge was recorded on 5 December 2013 as the storm *Xaver* also crossed the North Sea. The predictability of heights based on the British tide gauges is higher in Texel than in Cuxhaven. For both locations, the height is closer related to the height in Immingham than in Aberdeen. The ratios of heights $\frac{h_{Tex}}{h_{Imm}}$ and $\frac{h_{Cux}}{h_{Imm}}$ show three times the variance in Cuxhaven, compared to Texel. In Texel, only seven of the 101 external surges are recorded higher than in Immingham with a maximum increase of 17 cm. These growing surges reach heights between 58 cm and 103 cm in Texel. An increase of heights

395   between Immingham and Cuxhaven is also rare but more prevalent with 20 % of the events showing a height increase. Among those are two of the highest recorded surges, reaching 148 cm and 121 cm. The closer correlation between Immingham and Texel can be explained by the shorter distance and minimizing the potential for currents or local weather influencing the surge height.

4.2 Classification based on meteorological conditions
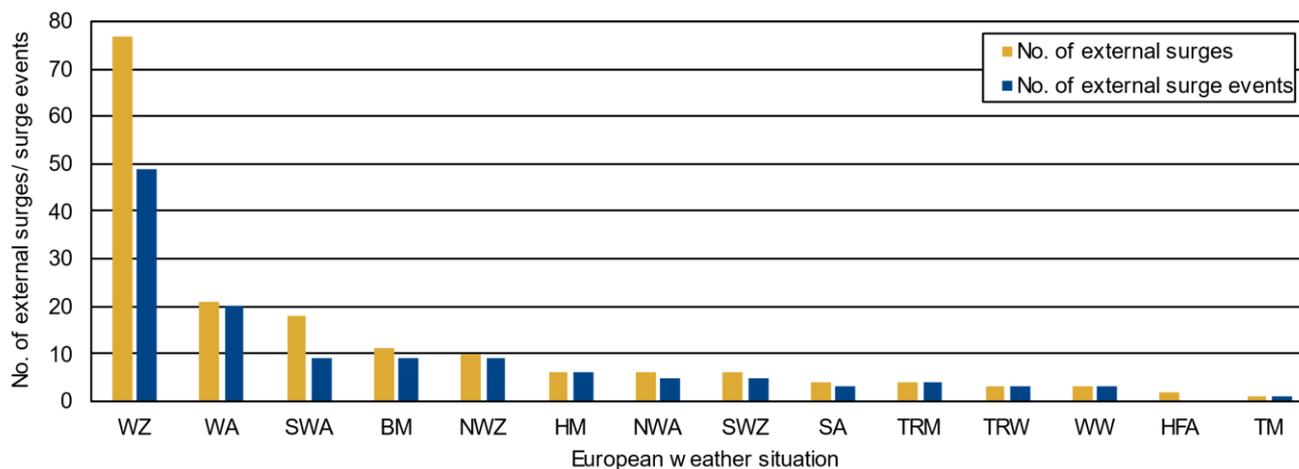
400

Figure 11: Number of external surges per European weather situation of the 1971 to 2020 external surges. Weather situations are defined by Hess and Brezowski (1977). The weather situation of an external surge is the one that is present at the date of arrival at Aberdeen. For an external surge event, the weather situation of the first or only surge in the series is used. For the weather situation HFA, no external surge event is noted, as both external surges occurred as part of a series that started during a different weather

405   **situation.**

The occurrence of external surges in the North Sea basin is strongly coupled to storm systems in the North Atlantic. Although the process of the physical meteo–oceanic coupling is not within the scope of this work, it will be important to correlate the

observations from the tide gauge data to general weather pattern. To briefly repeat meteorological conditions in a context of surge generation, the European weather situations during the beginning of the observed external surges (DataSet1+DataSet2) are assembled first. The European weather situations were originally defined by Hess and Brezowski (1977) and determined by Werner and Gerstengarbe (2010) for the duration from 1881 to 2009. From 2010 onwards, the records from German Meteorological Service (2021) are used.

Figure 11 correlates the weather situations as per Hess and Brezowski (1977) definition with the number of external surges that were detected at the time of the weather situation. The Agency for Roads, Bridges and Waters Hamburg (2012) already collected the weather situations during the 1971 to 1995 and found that the weather situation "Western situation cyclonic" (WZ) produces by far the most external surges with about half of the external surges being recorded during this weather situation. The three other main weather situations that were found during external surges are "Western situation anticyclonic" (WA), "South–western situation anticyclonic" (SWA) and "High–pressure bridge Central Europe" (BM). Including the 1995 to 2020 dataset (DataSet2), an additional main weather situation prone to generating external surges is however now identified: "North–western situation cyclonic" (NWZ). From only three external surges in the older dataset, the number of external surges during this weather situation more than doubles in DataSet2. Two other weather situations show an increase in significance: BM and SWA. Meanwhile, the share of external surges caused during the weather situations WZ and WA slightly lost significance. Still, these variations lie within the natural variance of the occurrence of external surges.

Table 6: Number of serial external surges depending on the number of external surges in the series and the number of weather situations during the start of the contained external surges.

Number of external surges in the series	Number of weather situations during the series		
	1	2	3
2	15	4	0
3	3	5	0
4	1	0	1
5	0	0	0
6	1	0	0
Σ	20	9	1

Serial external surges seem to be more prevalent during certain weather conditions, namely WZ and SWA situations, which show the highest rations of external surges to the number of external surge events. They seem to also be supported by long lasting weather situations. Table 6 shows that 20 of the 30 serial events did not happen during changing weather situations, including the series of six external surges, and only one event (consisting of four external surges) was driven by three different weather situations. These observations are based on a rather small sample size, so they should be assessed by further, more detailed studies of the weather conditions that cause external surges, for example the analysis of travel paths of the low–pressure cells.

The characteristics of the weather situations can be summarized from Werner and Gerstengarbe (2010) with respect to low
435   pressure cells:

- **WZ**: Single disturbances with high–pressure cells in between travel from Ireland over the British Isles, North and Baltic Sea towards Eastern Europe. The driving low–pressure cells is located north of 60° N.
- **WA**: The central low–pressure cell is often located north of 65° N with single disturbances travelling from west of Scotland over Scandinavia towards the Baltic.
440 - **SWA**: Low–pressure system is mostly located over the middle of the North Atlantic and the western Norwegian Sea. Single disturbances travel to the northeast.
- **NWZ**: Extensive low–pressure area over Scotland, the Norwegian Sea and Scandinavia with single disturbances travelling over the British Isles towards eastern Central Europe.
- **BM**: A high–pressure bridge between the Azores and Eastern Europe with an eastward directed frontal zone north of
445   it and single disturbances travelling eastwards.

These five weather situations show the characteristics that were previously associated with external surges in the North Sea with low–pressure cells over the North Atlantic and disturbances travelling eastwards and account for more than 80% of the detected external surges. The weather situation also influences the average height of the external surges with the highest occurring during WZ and BM conditions with 57 cm at Aberdeen and the lowest during the SWA situation only reaching
450   51 cm.

4.3 Combined events of external surge and storm surge events

Increased water levels caused by external surges along the North Sea coast are of particular interest if it comes to co–occurrence with storm surge events. Storm surge events, in most cases, are composed of tide and wind surge. Combined events of tide, wind surge and external surges have the potential to cause extreme water levels along the North Sea coast, challenging current
455   and future coastal protection strategies and actions. Therefore, analysing combined events of external– and storm surges is an essential step.

Table 7: Number of external surges and external surge events during storm surges.

No.	Name	External surge events, containing			Total events	External surges
		1 surge	2 surges	≥ 3 surges		
1)	Simultaneously with storm surge	13	4	4	21	31
2)	Without storm surge	83	15	7	105	141
3)	Total	96	19	11	126	172
4)	Percentage 1) of 3)	13.5 %	21.1 %	36.4 %	16.7 %	18.0 %

Combined events of external surge and storm surge events can be generated by two different meteorological situations: on the
460   one hand, both phenomena are initiated by two different extra–tropical cyclones in close succession. Due to different
propagation velocities both phenomena arrive at a tide gauge at the same time. On the other hand, both phenomena are initiated
by the same extra–tropical cyclone (Gönnert & Gerkensmeier 2015). Whether the wind set up is defined as storm surge or not
depends on the chosen definition these events. For this analysis, storm surges are defined as events reaching peaks of at least
+1.5 m above mean high water in Cuxhaven or a wind set up of at least 2 m is reached independent to the tidal phase (definition
465   follows the determination of Agency for Roads, Bridges and Waters Hamburg (2012), who is responsible for assessing the
design water level for public coastal protection facilities of the Free and Hanseatic city of Hamburg).

Following this definition, 21 or 16.7 % out of 126 external surge events recorded between 1971 and 2020, occurred during or
close to a storm surge event in the German Bight. Moreover, serial external surge events, a phenomenon that was analysed in
this study for the first time, can be observed more frequently during combined events. Particularly the number of external
470   surges in the series increases during combined events, compared to observed single events (cf. Table 7). As stated before, the
statistical correlations have to be verified by further research about the interactions of external and storm surges.

Findings presented above already underline the need to further investigate the phenomenon of serial external surge events, as
they might play an important role to determine the maximum range of combined extreme events, applied for example for
determination of design level heights. It can be assumed that higher quantities of extreme events during a serial external surge
475   event increase the potential for an unfavourable superposition of storm surge and external peaks. Hence, this requires
consideration of the increased time span of serial external surges (compared to the time span of combined events with one
external surge) in the determination of design standards. Further insights on meteorological conditions, causing combined
events including a serial external surge event, as well as improved knowledge about propagation velocity of external surges
are needed at this point.

480   With regard to a more detailed analysis of the average height of the external surges during storm surge events, DataSet2 shows
an increase to an average of 64 cm in Aberdeen and 70 cm in Cuxhaven (compared to average heights without storm surges of
56 cm in Aberdeen and 60 cm in Cuxhaven as described in Sect. 4.1). It confirms former findings for average heights of
external surges during storm surge events compiled for DataSet1 (1971–1995) (Agency for Roads, Bridges and Waters
Hamburg, 2012). Local effects of the extra–tropical cyclones involved during the development of these combined events might
485   play a role in this development. One special example of an external surge occurring during a storm surge is the external surge
during the storm *Xaver* on 5 and 6 December 2013. The external surge, which was earlier detected by Fenoglio–Marc et al.
(2015) using satellite altimetry, contributed to record water levels at some parts of the German coast (Dangendorf et al., 2016)
and, in the present study, reached a calculated height of 146 cm at the Cuxhaven tide gauge. Upon closer inspection, this
calculation was most likely influenced by missing wind records at some German weather stations, bringing the maximum
490   height to 95 cm. Still, extraordinary heights were calculated at Immingham and Texel (Spencer et al., 2015; Kettle, 2020),
highlighting the need for further, detailed analysis of single external events using multiple approaches to assess the occurrence
and impact of the highest external surges.

5 Discussion

The automated detection of external surges presented in this study, improves the possibility of faster and more detailed analysis
of external surges, while past work had predominantly relied on manual interpretation of tide records. Using the automated
algorithm (cf. Sect. 3.3), further tide gauges can be easily added to get a more detailed picture of heights, timing and velocity
of external surges and analysis might be expanded to the Danish or Norwegian coast. Moreover, for the first time, active
application of the automated algorithm facilitates a continuous monitoring of external surge events. A reanalysis of the 1971
to 1995 period might also be possible and meaningful to find deviations due to the changes in the detection, but data
assimilation and pre–processing is more time consuming due to the increased temporal resolution. Additional characteristics
of the external surges can also be analysed in future studies using the new dataset. For example, the meteorological conditions
used in this study only resemble generalized classification. Analysis of the tracks of the low–pressure cells is important to
understand their influence on the generation, propagation, and surge characteristics. Combination with the analysis of storm
tracks (e.g. Ganske et al., 2018; Horsburgh et al., 2021) is important to identify possible extreme events consisting of external
surges and storm surges. Moreover, the enhanced dataset can be used to evaluate the time of arrival of external surges at certain
tide gauges in relation to tides and the maximum wind setup to further investigate non–linear interactions.

By providing an adapted methodological approach, application of the study disclosed further points for improvements with
regard to detailed analysis of the characteristic of external surge events. This study showed a significant number of events
similar to external surges with an offset larger than 6 h between Aberdeen and Immingham that are not yet considered in the
dataset. Those events still need to be verified as external surges, for example by numerical models and assessment of weather
conditions. With regard to the measured height of external surges, which is strongly related to the height of the wind setup,
this study used a simplified version of the hindcast method by Müller–Navarra and Giese (1999). A more complex approach,
such as hindcast modelling of all relevant storm conditions, might improve the accuracy of the overall analysis. For this
improvement, the predictors of Müller–Navarra and Giese (1999) have to be split into those that are independent of external
surges and those influenced by them. Predictors like the residual at Aberdeen and residual spanning multiple tide phases can
be included to separate local and far field meteorological effects. They should, however, only be included during the
determination of the regression factors, not in the calculation of wind setup. This way the effect of external surges on the
regression is minimized but external surges remain part of the residual. On the other hand, to better predict values between
tide peaks and to quantify non–linear interactions, the height of the tide could be added as an additional predictor. Moreover,
further improvement to increase the level of specification of the external surge heights could be reached by improving the
hindcast method suitable for the British tide gauges. Using a modified set of predictors and suitable location for the wind data
should produce results similar to those of Rossiter (1959), as he also used MLR to determine the optimal weights in his forecast.
An accurate hindcast of wind setup at these locations could on one hand improve the accuracy of the measured height and on
the other hand enable a smaller height threshold for the detection of external surges, resulting in a more detailed dataset for
future analysis.

Natural Hazards
and Earth System
Sciences
Discussions

EGU
Open Access

The combination of the manually compiled DataSet1 from 1971 to 1995 and the new DataSet2 spanning the 1995 to 2020 period provides further insight into the occurrence of external surges in the North Sea and their variability on a decadal perspective. Findings resulting from the improved dataset can also be used to assess existing procedures how to deal with extreme water levels; and therewith have a direct effect of coastal protection in practice. In the particular case of the free and

530 hanseatic city of Hamburg the responsible authority, the Agency for Roads, Bridges and Waters (LSBG) is one of the few, who explicitly considers external surges as an essential component of extreme water level events in their assessment (Gönnert and Müller, 2014). The design level height is determined by a multi–method approach that analyses and includes non–linear interactions of all storm surge components (spring tide, wind surge and external surge). These non–linear interactions with spring tides and wind setup reduce the effective height of an external surge (Gönnert et al., 2010). The resulting design level

535 height in Hamburg incorporates an external surge with a height of 77 cm that results from the highest observed external surge reached at tidal gauge Aberdeen (1.08 m) and a determined reduction of 30% on its way to Cuxhaven, due to non–linear interactions with a very high wind surge during an extreme storm surge event (Gönnert et al., 2010; Agency for Roads, Bridges and Waters Hamburg, 2012). The extended dataset provided the opportunity for the LSBG to verify the assumptions for external surges in its design level concept for an even longer period. Thus, possible, necessary adjustments of the assumption

540 of a maximum height of external surges in the context of an extreme storm surge event described above had be examined and confirmed.

However, this study highlighted the need to assess serial external surges, a phenomenon that was found during the analysis of external surges in this study, more thoroughly in the future, particularly as it might alter the design assumptions regarding long–lasting (extreme) water levels stretching a couple of tidal cycles causing increased stress on coastal protection facilities.

545 **6 Conclusion and outlook**

External surges are an important component of extreme water levels in the North Sea. To improve the knowledge on their impact, this study conducted has come to the following conclusions, which the authors have briefly combined with relevant aspects for future research:

- This work has successfully improved and implemented an automated detection algorithm of external surges within
550 water level time histories. The automation improves the flexibility of the analysis to add further tide gauges or additional timespans. Comparative studies with similar phenomena in other shelf seas will now be possible, should more data become available in these areas. Modification of the automated detection should however be tested for the accurate detection of those phenomena in other pilot regions than the North Sea.

- The most important characteristics of external surges in the North Sea from 1995 to 2020 like their height, seasonality
555 and connection to European weather conditions and storm surges were presented an analysed. The most important novel finding is the occurrence of serial external surges, meaning multiple external surge that arrive at a tide gauge

less than three days apart. For this definition, statistical, meteorological, and hydrodynamic factors are taken into account. 33 % of the external surges that occurred between 1995 and 2020 are part of a series of external surges.

- The novel methods of detection adapt those of Gönnert (2003), so that her dataset and the newly derived events can be combined to span almost 50 years of external surge records containing 172 external surges. The findings of this study align with those of Gönnert (2003) and the variance is within the margin of natural variability. The larger, combined dataset enables further analysis of external surges and non–linear interactions with tide and wind setup. However, the combined dataset is still too small to allow the reliable analysis of long–term trends spanning decades to centuries. Hence, there is a need for continuous monitoring of external surges.

- The discussion of the enhanced dataset in the practical context of design level heights confirmed no relevant changes due to external surge heights compared to DataSet1 have to be considered for the design level concept in Hamburg, Germany. From a more general perspective, the study emphasizes consideration of the phenomenon of serial external surge events in the design level practice, as they might cause increased impact on coastal protection facilities as well as it might cause challenges due to increased surge induced blockage of estuarine inflow. Both might require future adaptation of coastal protection and risk management strategies.

Focusing on these aspects and proposing specific questions, this study demonstrates the need for further research on external surges in consideration of changing climate conditions, coastal communities, and risk management strategies.

Code and data availability

Weather and tide gauge data are available through the cited sources. Codes and all other data are available upon reasonable request to the authors.

Author contributions

BG, GG & NG conceptualized the study. GG and AM developed and improved the methodology. AM implemented the code and curated the data. The investigation was conducted by AM & BG, formal analysis by AM, BB & CK. AM wrote the original draft, which was edited by BB, BG, CK, GG, NG & OM. GG & NG supervised the project. NG provided a share of funding through a start–up grant of Technische Universität Braunschweig.

Competing interests

The authors declare that they have no conflict of interest.

Natural Hazards
and Earth System
Sciences
Discussions

Disclaimer

References

590 ABPmer: Atlas of UK Marine Renewable Energy Resources, http://www.renewables-atlas.info/, last access: 3 June 2022, 2008.

Agency for Roads, Bridges and Waters Hamburg: Ermittlung des Sturmflutbemessungswasserstandes für den öffentlichen Hochwasserschutz in Hamburg: Berichte des Landesbetriebes Straßen, Brücken und Gewässer Nr. 12 / 2012, Hamburg, 2012.

595 Albrecht, F., Wahl, T., Jensen, J., and Weisse, R.: Determining sea level change in the German Bight, Ocean Dynamics, 61, 2037–2050, https://doi.org/10.1007/s10236-011-0462-z, 2011.

Annutsch, R.: Wasserstandvorhersage und Sturmflutwarnung, Der Seewart, 38, 185–204, 1977.

Bork, I. and Müller–Navarra, S.: MUSE Modellgestützte Untersuchungen zu Sturmfluten mit sehr geringen Eintrittswahrscheinlichkeiten: Teilprojekt: Sturmsimulation, BSH, Hamburg, 2005.

600 Brown, J. M. and Wolf, J.: Coupled wave and surge modelling for the eastern Irish Sea and implications for model wind–stress, Continental Shelf Research, 29, 1329–1342, https://doi.org/10.1016/j.csr.2009.03.004, 2009.

Comer, J., Olbert, A. I., Nash, S., and Hartnett, M.: Development of high–resolution multi–scale modelling system for simulation of coastal–fluvial urban flooding, Nat. Hazards Earth Syst. Sci., 17, 205–224, https://doi.org/10.5194/nhess-17-205-2017, 2017.

605 Corkan, R. H.: The levels in the North Sea associated with the storm disturbance of 8 January 1949, Phil. Trans. R. Soc. Lond. A, 242, 493–525, https://doi.org/10.1098/rsta.1950.0008, 1950.

Corkan, R. H.: Storm Surges in the North Sea: Vol. 1 & 2, Washington D.C., 1948.

Dangendorf, S., Arns, A., Pinto, J. G., Ludwig, P., and Jensen, J.: The exceptional influence of storm 'Xaver' on design water levels in the German Bight, Environ. Res. Lett., 11, 54001, https://doi.org/10.1088/1748-9326/11/5/054001, 2016.

610 Darbyshire, J. and Darbyshire, M.: Storm Surges in the North Sea during the Winter 1953–4, Proc. R. Soc. Lond. A, 235, 260–274, https://doi.org/10.1098/rspa.1956.0081, 1956.

Dibbern, S. and Müller–Navarra, S.: Wasserstände bei Sturmfluten entlang der nordfriesischen Küste mit den Inseln und Halligen, Küste, 76, 205–224, 2009.

Dogan, G. G., Pelinovsky, E., Zaytsev, A., Metin, A. D., Ozyurt Tarakcioglu, G., Yalciner, A. C., Yalciner, B., and

615   Didenkulova, I.: Long wave generation and coastal amplification due to propagating atmospheric pressure disturbances, Nat Hazards, 106, 1195–1221, https://doi.org/10.1007/s11069-021-04625-9, 2021.

DWD Climate Data Center: Hourly measurements of wind and air pressure for Gemany, Version v21.3: Station Cuxhaven, DWD Climate Data Center, cdc.dwd.de, last access: 11 October 2021, 2021.

EMODnet Bathymetry Consortium: EMODnet Digital Bathymetry (DTM 2020), 2020.

620   Federal Maritime and Hydrographic Agency: Predicted tidal data: Station Cuxhaven–Steubenhöft, 2021.

Fenoglio–Marc, L., Scharroo, R., Annunziato, A., Mendoza, L., Becker, M., and Lillibridge, J.: Cyclone Xaver seen by geodetic observations, Geophys. Res. Lett., 42, 9925–9932, https://doi.org/10.1002/2015GL065989, 2015.

Fox–Kemper, B., Hewitt, H. T., Xiao, C., Aðalgeirsdóttir, G., Drijfhout, S. S., Edwards, T. L., Golledge, N. R., Hemer, M., Kopp, R. E., Krinner, G., Mix, A., Notz, D., Nowicki, S., Nurhati, I. S., Ruiz, L., Sallée, J.–B., Slangen, A.B.A., and Yu,

625   Y.: Ocean, Cryosphere and Sea Level Change, in: Climate Change 2021: The Physical Science Basis. Contribution of Working Group I to the Sixth Assessment Report of the Intergovernmental Panel on Climate Change, edited by: IPCC, Cambridge University Press, Cambridge, United Kingdom and New York, NY, USA, 1211–1362, https://doi.org/10.1017/9781009157896.011, 2021.

Ganske, A., Fery, N., Gaslikova, L., Grabemann, I., Weisse, R., and Tinz, B.: Identification of extreme storm surges with

630   high–impact potential along the German North Sea coastline, Ocean Dynamics, 68, 1371–1382, https://doi.org/10.1007/s10236-018-1190-4, 2018.

German Meteorological Service: Großwetterlagen ab 2003, Offenbach a.M., 2021.

Gönnert, G.: Storm tides and wind surge in the German Bight: Character of height, frequency, duration, rise and fall in the 20th Century, Küste, 185–366, 2003.

635   Gönnert, G. and Gerkensmeier, B.: A Multi–Method Approach to Develop Extreme Storm Surge Events to Strengthen the Resilience of Highly Vulnerable Coastal Areas, Coastal Engineering Journal, 57, 1540002-1-1540002-26, https://doi.org/10.1142/s0578563415400021, 2015.

Gönnert, G. and Müller, O.: Bemessung im Küstenschutz unter Berücksichtigung von Risikominderung und Klimaänderung, Geographische Rundschau, 30–38, 2014.

640   Gönnert, G., Gerkensmeier, B., Müller, J.–M., Sossidi, K., and Thumm, S.: Zur hydrodynamischen Interaktion zwischen den Sturmflutkomponenten Windstau, Tide und Fernwelle: Zwischenbericht Teilprojekt 1a, 114 pp., 2010.

Hess, P. and Brezowski, H.: Katalog der Großwetterlagen Europas 1881–1976, Deutscher Wetterdienst, Offenbach a.M., Berichte des Deutschen Wetterdienstes, 1977.

Horsburgh, K., Haigh, I. D., Williams, J., Dominicis, M. de, Wolf, J., Inayatillah, A., and Byrne, D.: "Grey swan" storm
645   surges pose a greater coastal flood hazard than climate change, Ocean Dynamics, 71, 715–730,
       https://doi.org/10.1007/s10236-021-01453-0, 2021.

Jong, M. P. C. de: Origin and prediction of seiches in Rotterdam harbour basins, 119 pp., 2004.

Kettle, A. J.: Storm Xaver over Europe in December 2013: Overview of energy impacts and North Sea events, Adv. Geosci.,
       54, 137–147, https://doi.org/10.5194/adgeo-54-137-2020, 2020.

650   Kim, H., Kim, M.–S., Lee, H.o.–J., Woo, S.–B., and Kim, Y.–K.: Seasonal Characteristics and Mechanisms of Meteo-
       tsunamis on the West Coast of Korean Peninsula, Journal of Coastal Research, 75, 1147–1151,
       https://doi.org/10.2112/SI75-230.1, 2016.

Kim, M.–S., Woo, S.–B., Eom, H., and You, S.–H.: Occurrence of pressure–forced meteotsunami events in the eastern
       Yellow Sea during 2010–2019, Nat. Hazards Earth Syst. Sci., 21, 3323–3337, https://doi.org/10.5194/nhess-21-3323-
655   2021, 2021.

Koninklijk Nederlands Meteorologisch Instituut: Uurwarden van weerstations: Station De Kooy, daggegevens.knmi.nl, last
       access: 1 October 2021, 2021.

Koopmann, G.: Wasserstandserhöhungen in der Deutschen Bucht infolge von Schwingungen und Schwallerscheinungen und
       deren Bedeutung bei der Sturmflut vom 16./17. Februar 1962, Deutsche Hydrographische Zeitschrift, 15, 181–198,
660   1962.

Kubota, T., Saito, T., Chikasada, N. Y., and Sandanbata, O.: Meteotsunami Observed by the Deep-Ocean Seafloor Pressure
       Gauge Network Off Northeastern Japan, Geophysical Research Letters, 48, https://doi.org/10.1029/2021GL094255,
       2021.

Liu, X., Jiang, W., Yang, B., and Baugh, J.: Numerical study on factors influencing typhoon–induced storm surge
665   distribution in Zhanjiang Harbor, Estuarine, Coastal and Shelf Science, 215, 39–51,
       https://doi.org/10.1016/j.ecss.2018.09.019, 2018.

Müller–Navarra, S. and Giese, H.: Improvements of an empirical model to forecast wind surge in the German Bight,
       Deutsche Hydrographische Zeitschrift, 51, 385–405, 1999.

NOC British Oceanographic Data Center: UK tide gauge network: Stations Aberdeen und Immingham, last access: 1
670   December 2021, 2021.

Olabarrieta, M., Valle–Levinson, A., Martinez, C. J., Pattiaratchi, C., and Shi, L.: Meteotsunamis in the northeastern Gulf of
       Mexico and their possible link to El Niño Southern Oscillation, Nat Hazards, 88, 1325–1346,
       https://doi.org/10.1007/s11069-017-2922-3, 2017.

Olbert, A. I. and Hartnett, M.: Storms and surges in Irish coastal waters, Ocean Modelling, 34, 50–62,
675   https://doi.org/10.1016/j.ocemod.2010.04.004, 2010.

Oppenheimer, M., Glavivic, B. C., Hinkel, J., Wal, R. v. d., Magnan, A. K., Abd–Elgawad, A., Cai, R., Cifuentes–Jara, M.,
       DeConto, R. M., Ghosh, T., Hay, J., Isla, F., Marzeion, B., Meyssignac, B., and Sebesvari, Z.: Sea Level Rise and

Natural Hazards
and Earth System
Sciences
Discussions

Implications for Low–Lying Islands, Coasts and Communities, in: The Ocean and Cryosphere in a Changing Climate, edited by: IPCC, Cambridge University Press, 321–446, https://doi.org/10.1017/9781009157964.006, 2019.

680 Ponte, R. M. and Gaspar, P.: Regional analysis of the inverted barometer effect over the global ocean using TOPEX/POSEIDON data and model results, J. Geophys. Res., 104, 15587–15601, https://doi.org/10.1029/1999JC900113, 1999.

Prandle, D.: Storm Surges in the Southern North Sea and River Thames, Proceedings of the Royal Society of London. Series A, Mathematical and Physical Sciences, 344, 509–539, 1975.

685 Proudman, J.: The Effects on the Sea of Changes in Atmospheric Pressure, Geophysical Journal International, 2, 197–209, https://doi.org/10.1111/j.1365-246X.1929.tb05408.x, 1929.

Proudman, J. and Doodson, A. T.: Time–Relations in Meteorological Effects on the Sea, Proceedings of the London Mathematical Society, s2-24, 140–149, https://doi.org/10.1112/plms/s2-24.1.140, 1926.

Rijkwaterstaat: Waterinfo: Water level and astronomical tide in cm above NAP: Tide gauge Texel Noordzee,
690 waterinfo.rws.nl, last access: 11 October 2021, 2021.

Rossiter, J. R.: Research on methods of forecasting storm surges on the east and south coasts of Great Britain, Q.J Royal Met. Soc., 85, 262–277, https://doi.org/10.1002/qj.49708536508, 1959.

Rossiter, J. R.: Storm Surges in the North Sea, 11 to 30 December 1954, Phil. Trans. R. Soc. Lond. A, 251, 139–160, 1958.

Schmitz, H.P., Habicht, D., and Volkert, H.: Barotropic numerical experimens on external surge generation at the edge of the
695 north-western European shelf, Gerland Beitr. Geophysik, 422–437, 1988.

Sibley, A., Cox, D., Long, D., Tappin, D., and Horseburgh, K.: Meteorologically generated tsunami-like waves in the North Sea on 1/2 July 2015 and 28 May 2008, Weather, 71, 68–74, https://doi.org/10.1002/wea.2696, 2016.

Spencer, T., Brooks, S. M., Evans, B. R., Tempest, J. A., and Möller, I.: Southern North Sea storm surge event of 5 December 2013: Water levels, waves and coastal impacts, Earth-Science Reviews, 146, 120–145,
700 https://doi.org/10.1016/j.earscirev.2015.04.002, 2015.

Steffelbauer, D. B., Riva, R. E. M., Timmermans, J. S., Kwakkel, J. H., and Bakker, M.: Evidence of regional sea-level rise acceleration for the North Sea, Environ. Res. Lett., 17, 74002, https://doi.org/10.1088/1748-9326/ac753a, 2022.

Tomczak, G.: Verification of a progressive wave in the southern north sea, Deutsche Hydrographische Zeitschrift, 11, 129–138, 1958.

705 Treloar, P., Taylor, D., and Prenler, P.: Investigation of Wave induced Storm Surge within a large Coastal Embayment - Moreton Bay (Australia), Proceeding of the Coastal Engineering Conference, 2010.

Vennell, R.: Resonance and trapping of topographic transient ocean waves generated by a moving atmospheric disturbance, J. Fluid Mech., 650, 427–442, https://doi.org/10.1017/S0022112009993739, 2010.

Vennell, R.: Long Barotropic Waves Generated by a Storm Crossing Topography, Journal of Physical Oceanography, 37,
710 2809–2823, https://doi.org/10.1175/2007JPO3687.1, 2007.

Vilibić, I.: Numerical simulations of the Proudman resonance, Continental Shelf Research, 28, 574–581, https://doi.org/10.1016/j.csr.2007.11.005, 2008.

Wahl, T., Haigh, I. D., Woodworth, P. L., Albrecht, F., Dillingh, D., Jensen, J., Nicholls, R. J., Weisse, R., and Wöppelmann, G.: Observed mean sea level changes around the North Sea coastline from 1800 to present, Earth-Science
715   Reviews, 124, 51–67, https://doi.org/10.1016/j.earscirev.2013.05.003, 2013.

Wasserstraßen– und Schifffahrtsverwaltung des Bundes: Water level data: Tide gauge Cuxhaven–Steubenhöft, Years 1995–1997, Federal Waterways and Shipping Administration (WSV), provided by Bundesanstalt für Gewässerkunde, last access: 11 October 2021, 2021a.

Wasserstraßen– und Schifffahrtsverwaltung des Bundes: Water level data: Tide gauge Cuxhaven–Steubenhöft, Years 1998–
720   2020, www.kuestendaten.de, last access: 12 October 2021, 2021b.

Werner, P. C. and Gerstengarbe, F.–W.: Katalog der Großwetterlagen Europas (1881-2009): Nach Paul Hess und Helmut Brezowsky, 7. verbesserte und ergänzte Auflage, PIK Report, 119, Potsdam, 2010.